**To cite this article:** GUO J, HU Z, ZHU Z W, et al. Numerical calculation and analysis of resistance performance of planing craft combining Savitsky method and overset grid technology[J/OL]. Chinese Journal of Ship Research, 2022, 17(3). http://www.ship-research.com/en/article/doi/10.19693/j.issn.1673-3185.02417.

**DOI:** 10.19693/j.issn.1673-3185. 02417

# Numerical calculation and analysis of resistance performance of planing craft combining Savitsky method and overset grid technology

*GUO Jun*[1], *HU Zhe*[1], *ZHU Ziwen*[1], *CHEN Zuogang*[*2,3], *CUI Lianzheng*[2,3], *LI Guibin*[4]

1 School of Marine Engineering, Jimei University, Xiamen 361021, China

2 State Key Laboratory of Ocean Engineering, Shanghai Jiao Tong University, Shanghai 200240, China

3 School of Naval Architecture, Ocean and Civil Engineering, Shanghai Jiao Tong University, Shanghai 200240, China

4 Science and Technology of Water Jet Propulsion Laboratory, Marine Design and Research Institute of China, Shanghai 200011, China

**Abstract:** [**Objective**] In this paper, the hydrostatic resistance of a planing craft is studied using the high-precision numerical simulation method to improve the numerical prediction accuracy. [**Methods**] The three-dimensional viscous flow field of a planing craft in calm water is numerically simulated using the computational fluid dynamics (CFD) method combined with the Savitsky method and overset grid technique, and the flow field characteristics of the craft under different load coefficients and speeds are analyzed. [**Results**] The calculated results of the resistance, sinkage, and trim angle of the planing craft are in good agreement with the experimental results, and the spray phenomenon and distribution of water and air at the bottom of the craft are simulated normally, which shows that this method can accurately and effectively predict the resistance performance of planing craft. With the increase in the load coefficient, the peak value of the pressure coefficient of on the keel increases, and the position of the pressure center moves forward. With the increase in speed, the peak value of the pressure coefficient on the keel decreases, and the position of the pressure center gradually moves towards the stern; the angle between the stagnation line and the longitudinal section of the center plane and the depth of the cavity behind the transom decrease, and the length of the cavity increases. [**Conclusions**] This study provides an accurate and effective numerical calculation method for the resistance prediction of planing craft, and can provide technical support for the numerical study of the hydrodynamic performance of such craft.

**Key words:** planing craft; resistance; computational fluid dynamics (CFD); overset grid; Savitsky method

**CLC number:** U661.31$^{+}$1

## 0 Introduction

As a high-speed craft that keeps in a planing state via the dynamic lift of the fluid that lifts the craft out of the water, a planing craft is featured by high speed and good mobility. Thanks to the excellent

**Received:** 2021 − 06 − 16 **Accepted:** 2021 − 09 − 14

**Supported by**: Educational and Research Projects for Young and Middle-Aged Teachers of Fujian Province of China (JAT200243, JAT190333); Project of Natural Science Foundation of Fujian Province of China (2021J05163)

**Authors:** GUO Jun, male, born in 1992, Ph.D., associate professor. Research interest: computational fluid dynamics of ships. E-mail: guojun6049@163.com

HU Zhe, male, born in 1988, Ph.D., professor. Research interest: R&D and application of ships and marine structures. E-mail: zhehu@jmu.edu.cn

ZHU Ziwen, male, born in 1991, Ph.D., lecturer. Research interest: computational fluid dynamics. E-mail: zwzhu@jmu.edu.cn

CHEN Zuogang, male, born in 1967, Ph.D., professor. Research interests: computational fluid dynamics of ships, and R&D and application of wind tunnels and circulating water channels. E-mail: zgchen@sjtu.edu.cn

***Corresponding author:** CHEN Zuogang

performance, planing craft has been applied in ships such as missile boats, torpedo boats, reconnaissance boats, traffic boats, and yachts, showing broad application prospects both in military and civilian fields. Given the significant changes in the attitude and drastic resistance variations during the whole navigation, it is of general interest among the researchers to explore how to predict the resistance performance of planing craft fast and accurately.

The early methods for predicting the resistance performance of planing craft mainly involve the semi-theoretical and semi-empirical formula method (e.g., the Savitsky method [1]), the atlas method based on test data on planing craft, and the resistance model test on planing craft. Among them, the prediction accuracy of the semi-theoretical and semi-empirical formula method and atlas method is subject to the similarity between the calculated ship type and its parent ship. Although the model test on planing craft can reflect intuitively the force on and flow field characteristics of the hull, it is costly and time-consuming. With the ongoing improvement in the computational accuracy of computational fluid dynamics (CFD), the use of the CFD technique can not only predict the force on and the motion of planing craft, but also capture the details of the flow field around the craft, which proves an economical and effective method for the study of the hydrodynamic problems of planing craft. In recent years, a growing number of researchers have used the CFD technique to conduct numerical simulations of planing craft and have achieved some results. Brizzolara and Serra [2] studied the accuracy of the CFD numerical simulation of the flow field of prismatic planing craft, the results of which showed that the CFD technique can be used to analyze and calculate the hydrodynamic problems of planing craft. Cao [3] predicted the full-scale ship resistance of planing craft at the fixed attitude by the software FLUENT, the result of which indicated that the calculation error was about 10%, and he believed that the software can predict the resistance of planing craft but cannot lead to ideal results in the prediction of the lift. Ghadimi et al. [4] adopted the RANS method to conduct a numerical simulation of the attitude of planing craft, and the results revealed that this method can be used for the preliminary design of planing craft. Ma et al. [5] carried out a numerical simulation of the resistance of planing craft by use of the mixed grid, and the results showed that there is some error between the results of numerical computation and those of the test. Jiang [6] numerically calculated the rapidity of a high-speed trimaran planing craft, the results of which demonstrated that the calculated resistance value is in good agreement with the test value at low speed, but the error between them would gradually increase with the rise in speed, which is about 30% at the maximum speed. Lotfi et al. [7] studied the hydrodynamic performance of a stepped planing craft by CFX, and the results showed that the prediction accuracy of resistance is about 5%. Frisk et al. [8] used FLUENT and STAR-CCM+ to make the numerical computation of the resistance and attitude of planing craft, the results of which suggested low resistance from the numerical prediction in the planing state and an inclination error of 32% in the semi-planing state. De Marco et al. [9] analyzed the hydrodynamics of planing craft via the overset grid technology and the deformation grid technology and found that the former performs better. Sun et al. [10] used STAR-CCM+ to explore the influence of three factors on the computational accuracy of resistance, convergence speed, and computational stability of prismatic planing craft, where the three factors refer to the height of the first-layer grid nodes on the hull surface, the scale of the grids on the hull surface, and the grid node distribution coefficient. Shao et al. [11] employed STAR-CCM+ to investigate the influence of time step and near-wall grid division on the computational accuracy of the resistance of planing craft, the results of which showed that both would affect the friction resistance of the planing craft and the water-air distribution at the bottom of the craft. Wei et al. [12] adopted NUMECA to conduct a numerical simulation on hydrofoil craft and found that the hydrofoil and spray rail can improve the resistance performance of the craft. Ding et al. [13] studied the influence of the factors such as the grid type and grid size on the water-air distribution, wave patten, hull attitude, and resistance at the bottom of planing craft in RANS computation and compared it with the results of the resistance test on the hull model. Yi et al. [14] explored the influence of the time step and grid number on the prediction results by use of FLUENT, CFX, and STAR-CCM+, and they found that some water volume fractions on the bottom surface of the planing craft simulated by CFX and STAR-CCM+ are about 0.5−0.8, and at the bottom of the craft, the preidcted volume fraction of water is low, with abnormal water-air distribution. They believed that a small time step and a

re-fined grid distribution can better the water-air distribution at the bottom of the craft. Li et al. [15] conducted a numerical simulation on the flow field around the planing craft via remodeling, the results of which showed that this method reports higher computational accuracy and efficiency than the overset grid method. Wang et al. [16] used the overset grid technology to simulate the wave-making of planing craft, the results of which indicated that the CFD method can accurately simulate the attitude of planing craft in calm water.

To sum up, although CFD technology can be used to predict the resistance performance of planing craft. However, there is an intense interaction between the planing hull and the fluid in the semi-planing and planing states, there are often water-air distribution anomalies at the bottom of the craft and difficulties in the simulation of the spray area in the numerical simulation. Moreover, there remains a significant error between the resistance prediction and the model test when the planing craft is in high-speed navigation. Therefore, it is necessary to further explore the methods for high-accuracy numerical prediction of the resistance of planing craft in the semi-planing and planing states. To this end, with the CFD method, this paper first uses the Savitsky method to estimate the attitude of a planing craft and then applies the overset grid technology to predict its resistance performance so as to provide an accurate and effective numerical prediction method for the resistance of planing craft. In addition, it also analyzes the effect of the attitude estimation of the planing craft on the resistance prediction. Then, the study carries out the numerical prediction of the resistance performance of planing craft in three load cases and at six speeds, the results of which are compared with the test results. Finally, it makes an analysis of the flow field characteristics of planing craft.

# 1 Computational model

In this paper, we take a model from model tests of planing craft conducted by Fridsma [17] in 1969 as the research object. The craft has a length of 1.143 m, a breadth of 0.228 6 m, a molded depth of 0.143 m, a displacement of 7.26 kg, and a deadrise angle of 10°. Fig. 1 presents the hull line and geometry model of the planing craft. The planing craft is divided into 20 stations along the length, with the lines from Station 2 to Station 20 the same and those from Station 0 to Station 2 shown in Fig. 1 (a), in which the numerical values show the stations in the line plan.

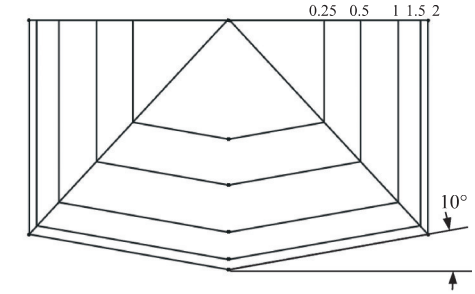


(a) Hull line

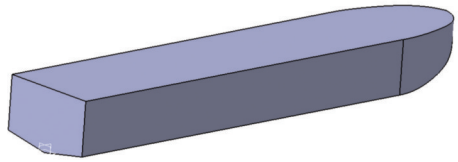

(b) Geometry model

Fig. 1 Geometry model of planing craft

The dimensionless speed of the planing craft is the volume Froude number $Fr_V$:

$$Fr_V = \frac{U}{\sqrt{gV^{1/3}}} \tag{1}$$

where $U$ is the speed of the planing craft; $g$ is the gravitational acceleration; $\nabla$ is the volume of displacement.

According to the difference of $Fr_V$, the motion of planing craft can involve three typical attitudes, i.e., the displacement state ( $Fr_V < 1.0$ ), semi-planing state, ($1.0 < Fr_V < 3.0$) and planing state ($Fr_V > 3.0$).

The load coefficient of the planing craft $C_V$ is defined as

$$C_V = \frac{\nabla}{B^3} \tag{2}$$

where $B$ stands for the breadth of the planing craft.

The different load conditions of the planing craft are presented in Table 1.

**Table 1 Load conditions of planing craft**

| Condition | Load coefficient | Draft/m | Longitudinal position of center of gravity/m | Vertical position of center of gravity/m |
|---|---|---|---|---|
| 1 | 0.304 | 0.026 | 0.400 | 0.067 |
| 2 | 0.608 | 0.042 | 0.457 | 0.067 |
| 3 | 0.912 | 0.057 | 0.457 | 0.067 |

# 2 Numerical calculation method

## 2.1 Computation method

We adopt the commercial software STAR-CCM+ for the numerical simulation of the hydrodynamic performance of the planing craft, with the basic equation for turbulent flow of the incompressible

fluid composed of the continuity equation and the momentum equation [18].

Specifically, the continuity equation can be written as

$$\frac{\partial u_i}{\partial x_i}=0 \tag{3}$$

and the momentum equation is

$$\frac{\partial u_i}{\partial t}+\frac{\partial}{\partial x_j}(u_iu_j)=-\frac{1}{\rho}\frac{\partial p}{\partial x_i}+\upsilon\frac{\partial}{\partial x_j}\left(\frac{\partial u_i}{\partial x_j}+\frac{\partial u_j}{\partial x_i}\right)+\frac{\partial}{\partial x_j}(-\overline{u_i'u_j'}) \tag{4}$$

where $u_i$ and $u_j$ are the time-average speed; $x_i$ and $x_j$ are the coordinates; $t$ is the time; $\rho$ is the fluid density; $p$ is the time-average pressure; $\upsilon$ is the viscosity coefficient of fluid motion; $-\overline{u_i'u_j'}$ is the Reynolds stress.

This paper adopts the SST $k$-$\omega$ turbulence model, which is often used for numerical computation of the hydrodynamic performance of ships, which can be expressed as [18]

$$\frac{\partial \rho k}{\partial t}+\frac{\partial \rho k u_i}{\partial x_i}=\frac{\partial}{\partial x_j}\left[\left(\mu+\frac{\mu_t}{\sigma_k}\right)\frac{\partial k}{\partial x_j}\right]+\tilde{G}_k-Y_k \tag{5}$$

$$\frac{\partial \rho \omega}{\partial t}+\frac{\partial \rho \omega u_i}{\partial x_i}=\frac{\partial}{\partial x_j}\left[\left(\mu+\frac{\mu_t}{\sigma_\omega}\right)\frac{\partial \omega}{\partial x_j}\right]+G_\omega-Y_\omega+D_\omega \tag{6}$$

where $\mu$ and $\mu_t$ are the dynamic viscosity coefficient and turbulence viscosity coefficient of the fluid, respectively; $\sigma_k$ and $\sigma_\omega$ are the turbulent Prandtl number of the turbulent kinetic energy $k$ and the dissipation rate $\omega$, respectively; $\tilde{G}_k$ and $G_\omega$ are the derivatives of $k$ and $\omega$, respectively; $Y_k$ and $Y_\omega$ are the dissipation term of $k$ and $\omega$, respectively; $D_\omega$ istands for the cross-diffusion term of $\omega$.

In the numerical calculation of the resistance of the planing craft, we adopt the volume of fluid (VOF) [19] method and the high-resolution interface capturing (HRIC) scheme to capture the free fluid surface, with the viscous solver based on separated flow as the solver, the SIMPLE method for the coupling of pressure and speed, and the second-order upwind scheme as the discrete scheme of the convection term. We also adopt the dynamic fluid-body interaction (DFBI) model to simulate the six degrees of freedom (6-DOF) motion of the craft that involves the freedom of sinkage and trim in the calculation, with the release time of the craft set as 0.5 s and the buffer time as 2.5 s. In addition, we use the implicit unsteady scheme, with the relationship between the time step $\Delta t$ of ship resistance and the length between vertical lines $L_{PP}$ and the speed $U$ presented as $\Delta t = (0.005-0.01)L_{PP}/U$ [20] in the numerical calculation recommended by International Towing Tank Conference (ITTC). The time step used in this paper for the resistance calculation of planing craft is $0.005L_{PP}/U$.

## 2.2 Computational domain and boundary conditions

As the geometry of the model and the flow field around it are generally symmetrical with respect to the longitudinal section of the center plane, the numerical simulation is aimed at half of the flow field around the planing craft. The computational domain and boundary conditions of numerical calculation are presented in Fig. 2. Specifically, the computational domain is composed of the static background domain and the overset domain that moves with the hull, and the overset grid method is adopted to deal with the problem of the significant changes in the hull attitude at high speed. The computational domain's length, breadth, and height are $13L_{pp}$, $5L_{pp}$, and $5L_{pp}$, respectively, with the speed inlet $2L_{pp}$ from the front of the craft and the top of the computational domain $1.0L_{pp}$ from the craft. We set the inlet, side, top, and bottom of the computational domain as the speed inlet boundary, the outlet of the domain as the pressure outlet boundary, and the hull surface as the no-slip wall boundary. In addition, we set a wave damping absorber in front of the out-

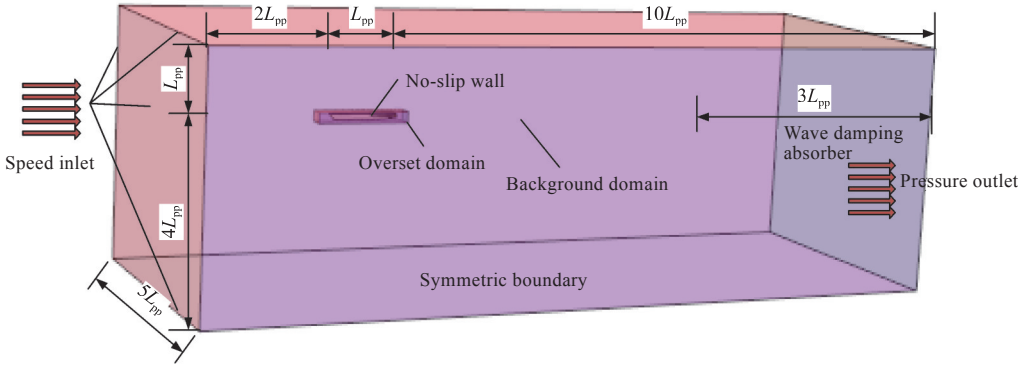


Fig. 2 Computational domain and boundary conditions

let of the computational domain to eliminate the ship wave transmitted to the outlet, and the damping length is $3L_{pp}$ to avoid wave reflection [21-22].

The grids are dissected and unstructured, and grid refinement around the planing craft and on the free surface is conducted. Moreover, we set three grid refinement areas taking the shape of the Kelvin wave patten around the craft for local refinement, three cuboid grid refinement areas at the design waterline for local refinement of the grids on the free surface, and one grid refinement area between the background domain and the overset domain for grid transition so that both domains share the same order of magnitude of grid size. The surface grid size of the craft is $1.75\%L_{PP}$, and the boundary layer grids of the craft are divided in the form of prism grids, which involve 15 layers in total, with a growth rate of 1.2. The thickness of the boundary layer $\delta$ is given by

$$\delta = 0.382 L_W Re_{L_W}^{-1/5} \tag{7}$$

where $L_W$ is the average wetted length of the planing craft; $Re$ is the Reynolds number.

The distributions of the free surface grids and the surface grids of the planing craft in the computational domain are shown in Fig. 3, where the number of grids in the background domain and the overset domain is 0.9 and 1.41 million, respectively, a total of 2.31 million grids in the computational domain.

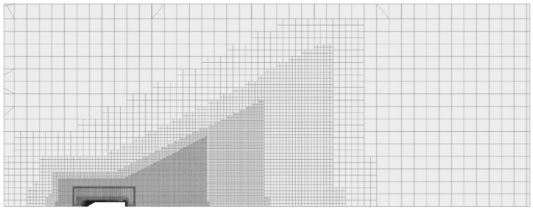

(a) Free surface grids

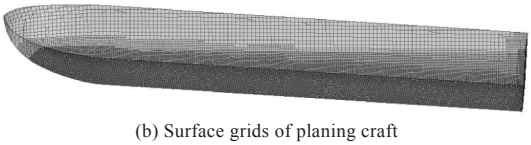

(b) Surface grids of planing craft

Fig. 3 Grids of computational domain

## 2.3 Attitude estimation

The hull attitude of planing craft in the displacement state is insignificantly different from that in the static floating state, while significant differences are reported between the hull attitude in the semi-planing state and planing state and that in the static floating state. Since the grids in the overset domain make bulk motion with the attitude variations of the planing craft, the area around the hull and the free surface needs a larger grid refinement area, which, however, will greatly increase the number of grids and lead to low computation efficiency. Therefore, adjusting the attitude of the planing craft to make the final calculated attitude close to the initial attitude upon the calculation can not only reduce the number of grids and raise computation efficiency, but also improve the convergence of the calculation. In addition, as the direction of the grids is close to that of the incoming flow, this can also alleviate the abnormality of water-air distribution at the bottom of the craft [23], thus improving the computational accuracy. In this paper, we adopt the semi-theoretical and semi-empirical formula, i. e., the Savitsky method [24-25], to estimate the attitude of the planing craft.

$$C_{L\beta} = \frac{F_{L\beta}}{0.5\rho U^2 B^2} = C_{L0} - 0.006\ 5\beta C_{L0}^{0.6} \tag{8}$$

where $C_{L\beta}$ is the lift coefficient; $F_{L\beta}$ is the lift (approximately equal to gravity in the planing state); $\beta$ is the deadrise angle; $C_{L0}$ is the lift coefficient at zero deadrise angle, and

$$C_{L0} = \theta^{1.1}(0.012\lambda_W^{0.5} + 0.005\ 5\lambda_W^{2.5}/Fr_B^2) \tag{9}$$

where $\theta$ is the trim angle of the planing craft; $\lambda_W$ is the average wetted length-breadth ratio; $Fr_B$ is the Froude number of craft breadth, and $Fr_B=U/(gB)^{0.5}$.

$$\frac{x_g}{\lambda_W B} = 0.75 - \frac{1}{5.21 Fr_B^2/\lambda_W^2 + 2.39} \tag{10}$$

where $x_g$ is the longitudinal distance between the center of gravity and the transom stern.

Upon the calculation, the initial attitude of the planing craft set under different load coefficients is presented in Fig. 4.

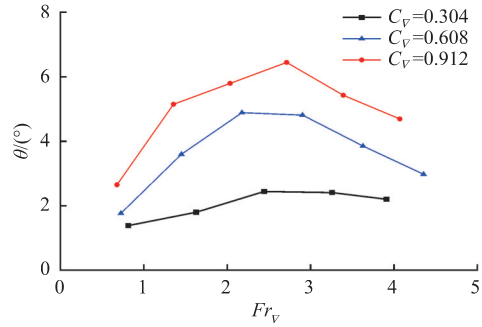


Fig. 4 Attitude estimation of planing craft

The total resistance coefficient $C_t$ of the planing craft is defined as

$$C_t = \frac{R_t}{0.5\rho A_{wet} U^2} \tag{11}$$

where $R_t$ is the total resistance of the planing craft; $A_{wet}$ denotes its dynamic wetted surface area.

Under the condition where the load coefficient

$C_V$= 0.608 and the speed $U$ = 4 m/s( $Fr_V$=2.904 ), we carry out the numerical calculation for the planing craft and analyze the influence of attitude estimation on its resistance prediction, with the comparison between the calculated results and the test results presented in Table 2 (in the table, $\sigma$ is the heave of the planing craft, and $L_{wet}$ is the wetted length). The prediction reports higher accuracy of the attitude, resistance, and wetted length of the planing craft via the Savitsky empirical formula combined with the overset grids for attitude estimation than that by mere use of the latter.

**Table 2 Influence of attitude estimation on resistance prediction**

| Method | $\sigma/B$ | $\theta$/(°) | $C_t$ | $L_{wet}/B$ |
|---|---|---|---|---|
| Test results (EFD) | 0.064 | 4.15 | 0.006 82 | 3.41 |
| Overset grid | 0.058 | 3.94 | 0.007 52 | 3.54 |
| Savitsky+overset grid | 0.060 | 4.07 | 0.007 25 | 3.47 |

# 3 Computed results

## 3.1 Computed results of resistance

Under three load conditions and six speeds ($U$ = 1, 2, 3, 4, 5, and 6 m/s), we numerically calculated the resistance performance of the planing craft and compared it with the results of the resistance test to verify the accuracy and effectiveness of the numerical method.

The comparison between the computed results (hereafter denoted as CFD results) and the test results (hereafter denoted as EFD results) of the heave of the planing craft is presented in Fig. 5. The computed sinkage is slightly small, and its average error in the three load conditions is 0.12%, 0.31%, and −5.06%, respectively. The comparison between the CFD results of the trim angle of the craft and the EFD results is shown in Fig. 6. The computed trim angle is slightly small, and its average error in the three load conditions is −0.62%, −2.11%, and −5.86%, respectively. The comparison between the CFD results of the total resistance of the craft and the EFD results shown in Fig. 7 indicates that the CFD results of resistance are over-estimated, and its average error in the three load conditions is 9.03%, 4.09%, and 6.93%, respectively. The comparison between the CFD results of the average wetted length of the craft and the EFD results shown in Fig. 8 demonstrates that the average error of wetted length in the three load conditions is −0.63%, 1.23%, and 1.61%, respectively. On the whole, the CFD results of the sinkage, trim angle, total resistance, and average wetted length of the planing craft are in good agreement with the EFD values, which shows the effectiveness of the numerical cal-

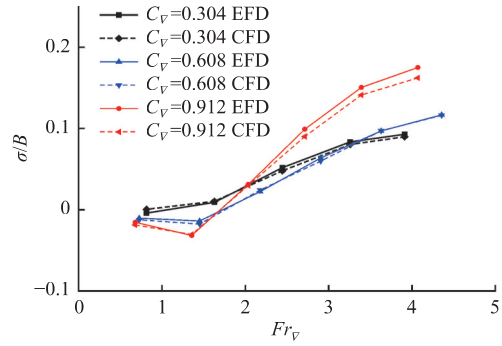


Fig. 5 Comparison between CFD and EFD results of heave

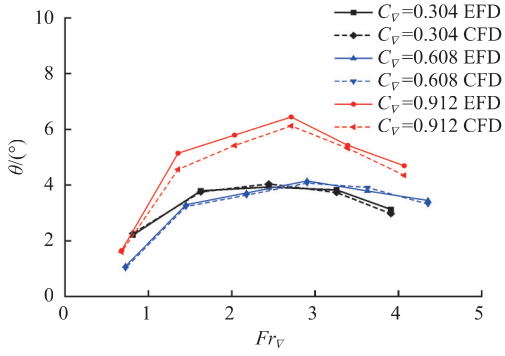


Fig. 6 Comparison between CFD and EFD results of trim angle

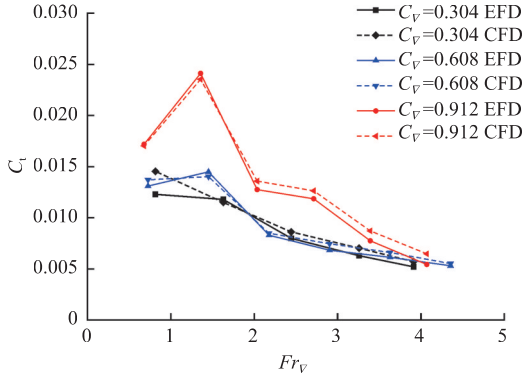


Fig. 7 Comparison between CFD and EFD results of resistance

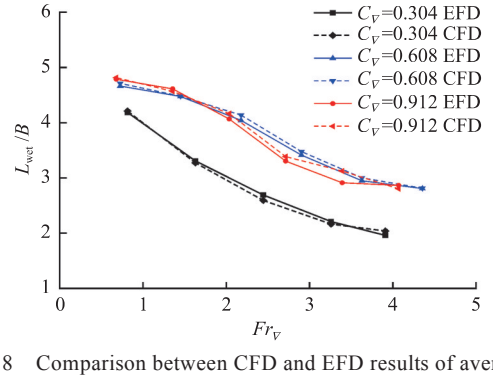


Fig. 8 Comparison between CFD and EFD results of average wetted length

culation method proposed in this paper and high accuracy and reliability of the CFD results. Thus, the method can be applied to the resistance prediction of the planing craft in the semi-planing and planing states.

### 3.2 Pressure distribution

The pressure coefficient of the planing craft $C_P$ is defined as

$$C_P = \frac{P - P_0}{0.5\rho U^2} \tag{12}$$

where $P$ is the absolute pressure on the surface of the planing craft, and $P_0$ is the pressure at the reference point (one atmosphere).

When the speed $U$ = 4 m/s, in different load conditions, the distribution laws of pressure on the surface of the planing craft are presented in Fig. 9, in which Fig. 9 (a) shows the pressure distribution of the keel of the craft, and Fig. 9 (b) represents the pressure distribution on the surface of the craft. In this figure, $x$ is the position along the direction of the length. It is indicated that the pressure coefficient of the keel increases significantly at places where it touches water, and then it reaches a peak at the stagnation point before decreasing to reach stability and gradually decreases to a negative value at the stern before reaching a minimum at the stern transom plate. When $C_V$=0.304, 0.608, the peaks of the pressure coefficient are relatively close, which makes the trim angle of the craft also relatively close; when $C_V$=0.912, the peak of the pressure coefficient increases, with the pressure center moving forward, which leads to the increase in the trim angle of the craft.

When the load coefficient $C_V$=0.912, the pressure distribution on the surface of the planing craft at different speeds is presented in Fig. 10. It is indicated that when $Fr_V$=1.357, the planing craft is at the initial stage of the semi-planing state, and in the spray area, the pressure coefficient first increases fast to the maximum, soon decreases to normal pressure subsequently, then slowly increases, and decreases fast to a negative value at the stern. When $Fr_V$ = 2.714, the craft is at the end stage of the semi-planing state, and the change laws of pressure distribution on the keel are generally the same as those in the planing state; with the increase in speed, the peak of the pressure coefficient of the stagnation point line decreases, and the line gradually moves towards the stern, with a smaller angle between the line and the longitudinal section of the center plane.

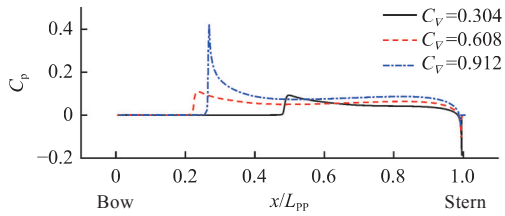


(a) Pressure distribution on keel

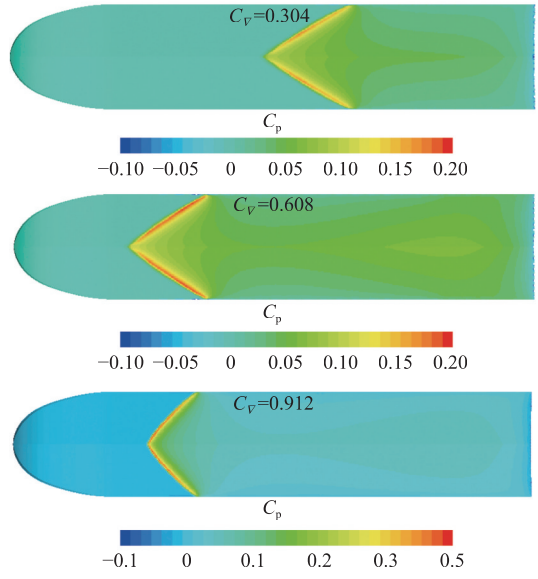


(b) Pressure distribution on hull surface

Fig. 9 Pressure distribution at different load conditions

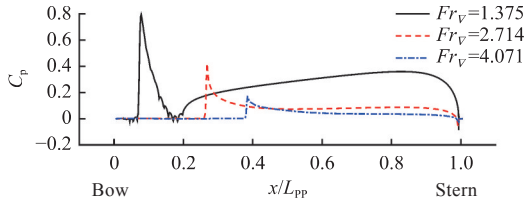


(a) Pressure distribution on keel

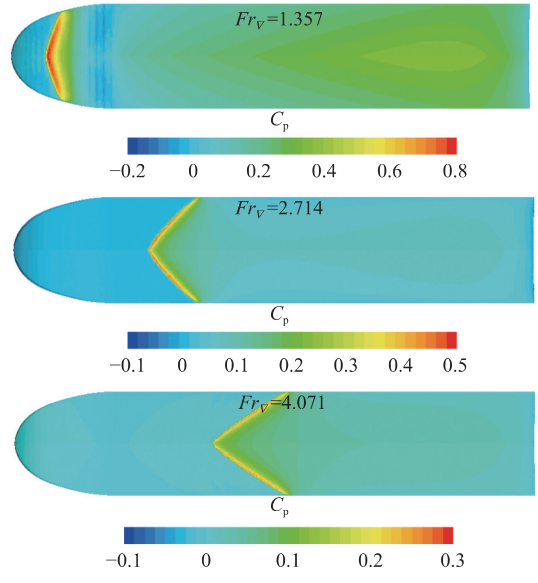


(b) Pressure distribution on hull surface

Fig. 10 Pressure distribution at different speeds

### 3.3 Free surface waveform

When the load coefficient $C_V$=0.912, the comparison of wave height on the free surface of the longitudinal section of the center plane of the planning craft at different speeds is presented in Fig. 11 (in the figure, $z$ is the wave height position of the free surface). The free surface waveform of the craft is shown in Fig. 12, in which the left figure presents the overall waveform, and the right one represents the waveform in the spray area. The increase in speed is accompanied by the gradual decrease in the angle of the ship wave and the height of the wave making at the bow and the rise in the height of the chicken-tail-shaped water mound behind the craft together with its backward movement. Moreover, the depth of the "cavity" behind the craft begins to fall accordingly, while the length of the "cavity" gradually increases. When $Fr_V$ =1.357, obvious spray occurs at the bow of the craft, and the water flow rolls forward after impacting the bow of the craft, which creates a large wetted area of spray. For $Fr_V$=2.714, spray occurs at the bottom of the hull, with the wetted shape of the spray area close to a triangle, and for $Fr_V$=4.071, the shape becomes completely triangular.

### 3.4 Water-air distribution

When the load coefficient $C_V$=0.912, the water-air distribution on the surface of the planing craft at different speeds is shown in Fig. 13. It is indicated from the figure that the volume fraction of the water phase in the contact part between the bottom of the craft and water is close to 1.0. This suggests a normal prediction of the water-air distribution at the bottom of the craft and no abnormality in its simulation, which also shows the accuracy of the numerically simulated resistance of the craft in this paper.

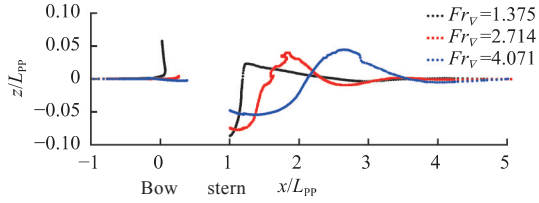


Fig. 11 Comparison of wave height on free surface of $y$ = 0 section at different speeds

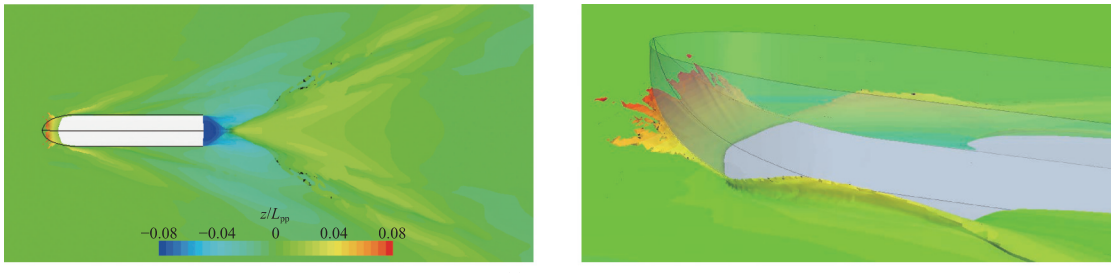


(a) $Fr_\nabla$=1.357

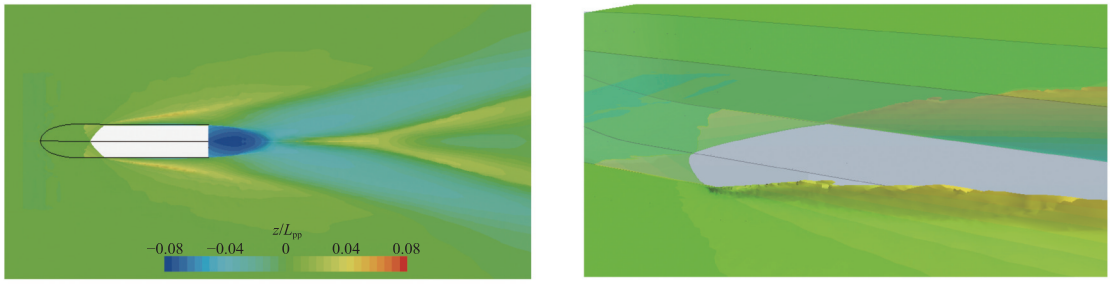


(b) $Fr_\nabla$=2.714

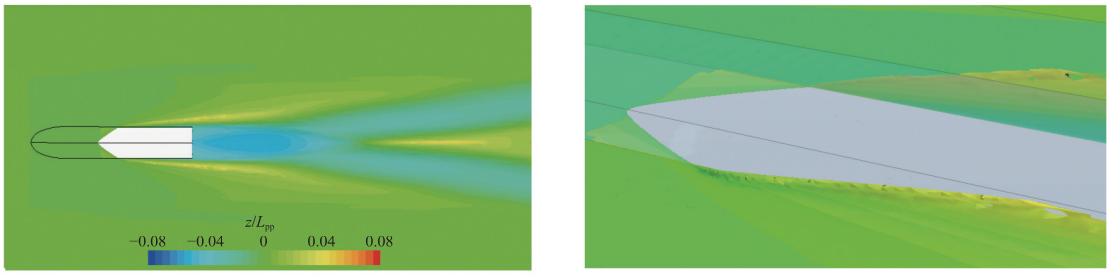


(c) $Fr_\nabla$=4.071

Fig. 12 Free wave surface distribution at different speeds

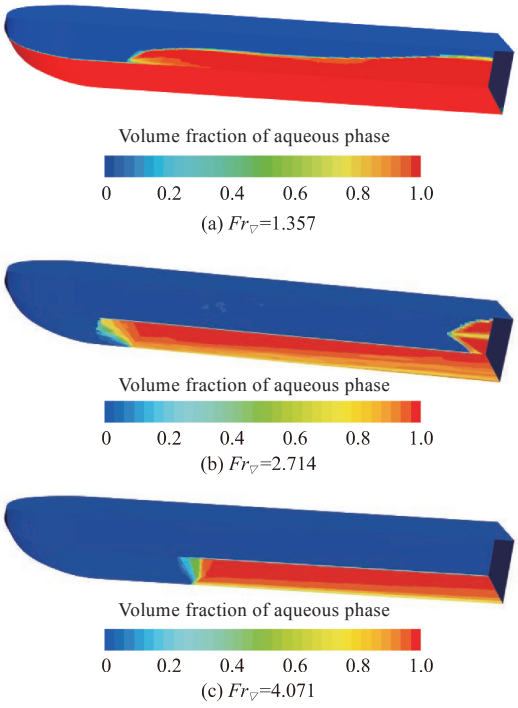


Fig. 13 Water-air distribution on the surface of planning craft at different speeds

## 4 Conclusions

Given the solution to the RANS equation, this paper first adopted the Savitsky method to estimate the attitude of a planing craft, then forecasted its resistance performance via the overset grid technique, and provided a high-accuracy method to numerically predict its resistance. Next, we predicted the resistance performance of the planing craft in three load conditions and compared it with the EFD results. Finally, we analyzed the flow field characteristics of the planing craft. Through the study, the following conclusions are drawn.

1) With the increase in the load coefficient, the peak coefficient of pressure on the keel begins to rise, and the pressure center moves forward; the trim angle of the planing craft also increases.

2) With the increase in speed, the peak coefficient of pressure on the keel falls; the stagnation point line gradually moves backward, and the angle between the stagnation point line and the longitudinal section of the center plane decreases. In addition, the angle of the ship wave of the planing craft gradually decreases; the wave making at the bow weakens, and the elevation of the chicken-tail-shaped wake at the stern increases; the depth of the "cavity" behind the craft decreases, but the length increases.

3) This paper gives a normal simulation of water-air distribution at the bottom of the planing craft, and the spray of the planing craft can be simulated. Moreover, the CFD results of the resistance of the planing craft are in good agreement with the EFD results. All these suggest that the numerical method in this paper is accurate and reliable, which can technically underpin the numerical study of the hydrodynamics of planing craft.

## References

[1] SAVITSKY D. Hydrodynamic design of planing hulls [J]. Marine Technology, 1964, 1 (4): 71−95.

[2] BRIZZOLARA S, SERRA F. Accuracy of CFD codes in the prediction of planing surfaces hydrodynamic characteristics [C]//2nd International Conference on Marine Research and Transportation, 2007.

[3] CAO H J. The computation and research on resistance of planing craft on the software FLUENT [D]. Harbin: Harbin Engineering University, 2008 (in Chinese).

[4] GHADIMI P, MIRHOSSEINI S H, DASHTIMANESH A, et al. RANS simulation of dynamic trim and sinkage of a planing hull [J]. Applied Mathematics and Physics, 2013, 1 (1): 6−10.

[5] MA W J, PANG Y J, SONG H W, et al. Application of mixed grid in numerical simulation of planning-hull resistance [J]. Ship Engineering, 2013, 35(4): 8−10, 58 (in Chinese).

[6] JIANG Y. CFD-based analysis on speed performance of high-speed trimaran planing boat [D]. Harbin: Harbin Engineering University, 2013(in Chinese).

[7] LOTFI P, ASHRAFIZAADEH M, ESFAHAN R K. Numerical investigation of a stepped planing hull in calm water [J]. Ocean Engineering, 2015, 94: 103−110.

[8] FRISK D, TEGEHALL L. Prediction of high-speed planing hull resistance and running attitude [D]. Gothenburg, Sweden: Chalmers University of Technology, 2015.

[9] DE MARCO A, MANCINI S, MIRANDA S, et al. Experimental and numerical hydrodynamic analysis of a stepped planing hull [J]. Applied Ocean Research, 2017, 64: 135−154.

[10] SUN H W, MA W J, ZHU J B. Research on grid factor in numerical calculation of planing craft resistance [J]. Shipbuilding of China, 2015, 56 (2): 170−178 (in Chinese).

[11] SHAO W B, MA S, DUAN W Y, et al. Calm-water resistance calculation of planing craft based on CFD method [J]. Ship Engineering, 2019, 41 (9): 41−45,137 (in Chinese).

[12] WEI Z F, JING S P, YANG S L. CFD simulation and comparison analysis of a new type high-speed boat [J]. Chinese Journal of Ship Research, 2016, 11 (4): 22−28 (in Chinese).

[13] DING J M, JIANG J B, QIN J T, et al. Influencing mesh factors in the calculation of the resistance performance of high-speed planing crafts through RANS [J]. Journal of Harbin Engineering University, 2019, 40

(6): 1065−1071 (in Chinese).
[14] YI W B, WANG Y S, PENG Y L, et al. Research on several influence factors in numerical prediction of planning craft resistance [J]. Journal of Huazhong University f Science and Technology (Natural Science Edition), 2017, 45 (9): 120−126 (in Chinese).
[15] LI Q N, QIN J T, ZHOU L L. Numerical calculation of planing boat resistance based on remesh method [J]. Ship Engineering, 2020, 42 (1): 42−46, 121 (in Chinese).
[16] WANG H, ZHU R C, YANG Y T, et al. Simulation and analysis of wave-making and attitudes of planing hull by CFD [J]. Shipbuilding of China, 2020, 61 (3): 1−14 (in Chinese).
[17] FRIDSMA G. A systematic study of the rough-water performance of planing boats. irregular waves-part II [R]. New Jersey: Davidson Laboratory Stevens Institute of Technology, 1969.
[18] WANG F J. Computational fluid dynamics analysis—principles and applications of CFD software [M]. Beijing: Tsinghua University Press, 2004: 7−12 (in Chinese).
[19] HIRT C W, NICHOLS B D. Volume of fluid (VOF) method for the dynamics of free boundaries [J]. Journal of Computational Physics, 1981, 39 (1): 201 – 225.
[20] ITTC. The specialist committee on CFD in marine hydrodynamics-recommended procedures and guidelines: practical guidelines for ship CFD applications [C]//Proceeding of the 26th ITTC. Rio de Janeiro, Brazil: ITTC,2011.
[21] GUO J, CHEN Z G, DAI Y X. Numerical study on self-propulsion of a waterjet propelled trimaran [J]. Ocean Engineering, 2020, 195: 106655.
[22] GUO J, ZHANG Y, CHEN Z G, et al. CFD-based multi-objective optimization of a waterjet-propelled trimaran [J]. Ocean Engineering, 2020, 195: 106755.
[23] LI K P, WEI C Z, LIANG X F, et al. Application of polyhedral mesh in numerical simulations of planing hulls [J]. Ship Science and Technology, 2020, 42 (2): 33−37 (in Chinese).
[24] SUN Y, LU X P, LI J Y, et al. Comparative study on simulation of resistance for planing craft [J]. Chinese Journal of Ship Research, 2019, 14 (1): 27−32 (in Chinese).
[25] FALTINSEN O M. Hydrodynamics of high-speed marine vehicles [M]. New York: Cambridge University Press, 2005: 516−530.

# 结合 Savitsky 方法和重叠网格技术的滑行艇阻力数值计算与分析

郭军[1], 扈喆[1], 朱子文[1], 陈作钢[*2,3], 崔连正[2,3], 李贵斌[4]
1 集美大学 轮机工程学院,福建 厦门 361021
2 上海交通大学 海洋工程国家重点实验室,上海 200240
3 上海交通大学 船舶海洋与建筑工程学院,上海 200240
4 中国船舶及海洋工程设计研究院 喷水推进技术重点实验室,上海 200011

**摘　要**：[**目的**]为提高数值预报精度,对滑行艇的静水阻力高精度数值模拟方法进行研究。[**方法**]应用计算流体动力学(CFD)方法,结合 Savitsky 方法和重叠网格技术,对滑行艇在静水中的三维黏性流场进行数值模拟,并对不同载荷系数和航速下滑行艇的流场特性进行分析。[**结果**]结果显示,滑行艇的阻力、升沉及纵倾角等计算结果与试验结果吻合良好,艇底的喷溅现象及水气分布模拟正常,表明采用所提方法可以准确、有效地预报滑行艇的阻力性能;随着载荷系数的增加,龙骨线压力系数的峰值增加,压力中心位置逐渐前移;随着航速的增加,龙骨线压力系数的峰值减小,压力中心位置逐渐后移,驻点线与中纵剖面的夹角减小,艇后"空穴"的深度减小、长度增大。[**结论**]所做研究可为滑行艇阻力预报提供一种准确、有效的数值计算方法,能为滑行艇水动力性能数值研究提供技术支撑。

**关键词**：滑行艇；阻力；计算流体动力学；重叠网格；Savitsky 方法